Journal of Nuclear Medicine, published on May 28, 2021 as doi:10.2967/jnumed.120.261854

^{131}Iodine-GD2-ch14.18 scintigraphy to evaluate option for radio-immunotherapy in patients with advanced tumors

Ying Zhang[1], Juergen Kupferschlaeger[1], Peter Lang[2], Gerald Reischl[3,4], Rupert J. Handgretinger[2], Christian la Fougère[1,4,5], Helmut Dittmann[1].

1 Department of Nuclear Medicine and Clinical Molecular Imaging, University Hospital Tuebingen, Otfried-Mueller-Strasse 14, 72076, Tuebingen, Germany.
2 Clinic for Paediatric Hematology and Oncology, University Hospital Tuebingen, Tuebingen, Germany.
3 Department of Preclinical Imaging and Radiopharmacy, University Hospital Tuebingen, Tuebingen, Germany
4 Cluster of Excellence iFIT (EXC 2180) "Image Guided and Functionally Instructed Tumor Therapies", University of Tuebingen, Germany
5 German Cancer Consortium (DKTK). Partner Site Tuebingen, Germany

Word count: 4921 words.

Running title: ^{131}I-GD2-scintigraphy before RIT

Corresponding author:

Ying Zhang, PhD
Eberhard-Karls-University Tuebingen
Department of Nuclear Medicine and Clinical Molecular Imaging
Otfried-Mueller-Str. 14, 72076 Tuebingen, Germany
Phone +49-7071-29-82164
Fax +49-7071-29-5869
E-mail: ying.zhang@med.uni-tuebingen.de

ABSTRACT

The tumor-selective ganglioside antigene GD2 is frequently expressed on neuroblastomas and to a lesser extent also on sarcomas and neuroendocrine tumors. Aim of our study was to evaluate tumor targeting and biodistribution of iodine-131-labeled chimeric GD2-antibody clone 14/18 (^{131}I-GD2-ch14.18) in patients with late-stage disease in order to identify eligibility for radioimmunotherapy. **Methods:** 20 patients (neuroblastoma n=9; sarcoma n=9; pheochromocytoma n=1, neuroendocrine tumor n=1) were involved in this study. 21 to 131 MBq (1-2 MBq/kg) of ^{131}I-GD2-ch14.18 (0.5-1.0 mg) were injected intravenously. Planar scintigraphy was performed within 1 h from injection (d0), on d1, d2, d3, and d6 or d7 to analyse tumor uptake and tracer biodistribution. Serial blood samples were collected in 4 individuals. Absorbed dose to tumor lesions and organs was calculated using Olinda® software. **Results:** The tumor targeting rate on a per-patient base was 65% (13/20) with 6/9 neuroblastomas showing uptake of ^{131}I-GD2-ch14.18. Tumor lesions showed maximum uptake at 20-64 h p.i. (effective half-life in tumors 33-192 h). The tumor absorbed dose varied between 0.52 and 30.2 mGy/MBq (median: 9.08, n=13). Visual analysis showed prominent blood pool activity up to d2/d3 p.i. No pronounced uptake was observed in the bone marrow compartment or in the kidneys. Bone marrow dose was calculated at 0.09-0.18 mGy/MBq (median: 0.12) while blood dose was 1.1-4.7 mGy/MBq. Two patients (1 neuroblastoma and 1 pheochromocytoma) with particularly high tumor uptake underwent radioimmunotherapy using 2.3 and 2.9 GBq of ^{131}I-GD2-ch14.18 both achieving stable disease. Overall survival was 17 and 6 months, respectively. **Conclusion:** ^{131}I-GD2-ch14.18 is cleared slowly from blood resulting in good tumor to background contrast not until 2 d after application. With acceptable red marrow and organ dose,

radioimmunotherapy is an option for patients with high tumor uptake. However, due to the variable GD2-expression, decision should be made depending on pretherapeutic dosimetry.

Keywords: Iodine-131-GD2, neuroblastoma, dosimetry, tumor dose, radioimmunotherapy

INTRODUCTION

The disialoganglioside GD2 is a sialic acid-containing glycosphingolipid physiologically expressed on cell surfaces in the central nervous system, peripheral sensory nerve fibers, and skin melanocytes at low levels (*1-3*). High GD2 expression has been recognized in tumors such as neuroblastoma (NB), bone and soft-tissue sarcoma, neuroendocrine tumors (NETs), and some brain tumors (*1,4*). Antibodies targeting GD2 have been shown to exert antibody-dependent as well as complement-dependent cytotoxicity in tumor cells (*1,5,6*). For tumor-specific therapy the chimeric antibody Dinutuximab (ch14.18) received approval with an orphan drug designation in 2015 from US Food and Drug Administration at a dose of 17.5 mg/m^2/day. It is the first monoclonal antibody specifically approved for maintenance treatment of pediatric patients with high-risk NB who have achieved at least partial response to first-line multimodal therapy. In patients with NB, Dinutuximab was shown to increase the 2-year event-free-survival rate from approximately 46% with standard treatment to 66% (*6-8*). Similar to this result, some patients with refractory or recurrent disease achieved benefit from an anti-GD2-therapy (*9-11*).

Radioimmunotherapy (RIT) also involves selective targeting of cancer-associated cell antigens, primarily using the antibody as a carrier vehicle for radionuclides that deliver irradiation to tumor areas (*12*). Thus, the anticancer activity of RIT is predominantly due to irradiation rather than antibody- or complement-dependent cytotoxicity. As a result, radiation sensitive tumors such as leukemia and lymphomas are good candidates for RIT. In particular, CD20-targeted RIT using ^{131}Iodine (^{131}I-tositumomab) (*13*) and ^{90}Yttrium- labelled antibodies (^{90}Y-ibritumomab-tiuxetan) (*14*) have demonstrated

durable remission of B-cell lymphoma. GD2 targeting RIT in high-risk NB patients first has been evaluated using the murine antibody 3F8 labelled with ^{131}Iodine (*15*). In the subgroup of patient receiving ^{131}I-3F8, the engraftment of autologous bone marrow transplantation was successful and long-term progression-free survival (PFS) was comparable to a combination therapy with 3F8 and GM-CSF for patients in first complete response (*16*).

Accurate patient stratification is of upmost interest, and there are a number of criteria that might help to identify eligibility for a RIT (*12*). Besides tumor specificity and high target antigen expression, low uptake of the radiolabelled antibody in organs like liver, spleen, and kidneys is crucial (*17*). Thus, evaluation of *in-vivo* biodistribution is a key step towards considering new applications of RIT (*18*).

Also with regard to potential adverse effects of immunotherapies like Dinutuximab, e.g. neuropathic pain, infusion reactions like hypersensitivity, hypotension, and occasionally capillary leak syndrome (*7,19*) it is highly desirable to identify eligibility (for immunotherapy and RIT) before taking decision of further treatment. Therefore, the aim of this pilot study was to evaluate tumor targeting and biodistribution of the ^{131}Iodine-labelled GD2-antibody ch14.18 (^{131}I-GD2-ch14.18) in patients with late-stage disease and ultimately identify candidates for RIT.

MATERIALS AND METHODS

Antibody preparation and radiolabelling

^{131}Iodine for labeling in sodium hydroxide solution was purchased from GE Healthcare Buchler (Braunschweig, Germany). The antibody GD2-mAb (ch14.18) in sterile aqueous solution (ca. 4–5 mg/mL) was provided by the childrens' hospital of our institution in quality for clinical trials. As iodination reagent, Iodo-Gen® (Thermo Fisher Scientific, Germany) was used. All other chemicals and materials were provided by commercial suppliers. According to supplier instructions, 200 µL of a solution (1 mg/mL) of Iodo-Gen® in CH_2Cl_2 were introduced per vial, followed by evaporation at room temperature. Coated vials were stored for a maximum of one week under inert gas in the dark.

For diagnostic application, 1–2 mg of antibody (200–400 µL of antibody solution) was added to a coated vial, followed by the acquired amount of ^{131}Iodine (25–100 µL) corresponding to 50–175 MBq. For therapeutic application, 5 mg of GD2-ch14.18 and 3000–4000 MBq ^{131}Iodine were used for the otherwise identical labeling procedure.

Patients and clinical characteristics

The need for written informed consent for this study was waived by the institutional review board (registry No. 821/2020BO2). Following the stipulations of the German medicinal products act ("Arzneimittelgesetz"; AMG §13(2b)) ^{131}I-GD2-ch14.18 was used in patients with late-stage disease and in order to identify candidates for RIT.

In total, 20 patients were included in this retrospective analysis (for details see Table 1). All patients had a history of surgical tumor resection and systemic chemotherapy. NB patients (eight children and one adult) suffered from stage IV disease and had

previously been treated by myeloablative chemotherapy with autologous hematopoietic stem cell rescue. Four out of nine patients additionally received external beam irradiation and 5/9 received non-radioactive GD2-antibody-therapy. All NB patients underwent ^{123}I-metaiodobenzylguanedin (^{123}I-MIBG)-scintigraphy which demonstrated tumor uptake in only 3/9 cases. Individuals with MIBG-positive tumors had earlier received ^{131}I-MIBG-therapy. Patients with metastatic sarcoma were predominantly adults (n= 6/9, age range 18-51 years). The remaining two patients suffered from advanced neuroendocrine tumor and malignant pheochromocytoma, respectively. MRI or CT imaging was used as reference standard for detection of tumor manifestations on ^{131}I-GD2-ch14.18 scans.

Protocol for scintigraphy

21 to 131 MBq (1-3 MBq/kg) of ^{131}I-GD2-ch14.18 (0.5-1.0 mg antibody) were diluted in 100 mL of 0.9% NaCl and infused intravenously over 45 to 60 minutes. Premedication included antihistamines and prednisolone. Whole-body planar scintigraphy was performed using a double head gamma camera (Hawkeye /Millenium VG®, GE Healthcare) with a high energy general purpose collimator and a matrix size of 1024 x 256 pixels. Energy window was set at 364 ± 36 keV for Iodine-131. Acquisitions were performed 1 h post-injection (p.i.), 24 h p.i., 48 h p.i., 72 h p.i. and if possible also 5-6 d p.i. Additional SPECT/CT of tumor regions was performed in some patients. Serial blood samples were collected from 4 patients (3 adults and 1 child).

^{131}I-GD2-ch14.18 -Treatment

Two adult patients (1 NB and 1 pheochromocytoma) received treatment with ^{131}I-GD2-ch14.18 (2275 MBq with 1.7 mg GD2-Ab and 2942 MBq with 1.6 mg GD2-Ab,

respectively). Comedications included dexamethasone 8 mg to 16 mg daily for 5 days, antihistamines and analgesia if required. Patients were hospitalized for 4-5 days after infusion. Post-treatment evaluations included clinical status, vital signs, neurologic examination, blood for serum chemistries, and ECG. Haemogram was controlled 0.5, 1, 2, and 3 months after treatment. Whole body (WB) CT imaging was performed 2 months and 5 months after treatment.

QUANTIFICATION AND DOSIMETRY

Normalized blood tracer concentration

Activity concentrations (Bq/mL) from blood samples (0.1-0.5 mL full blood) were determined using an automatic gamma counter (Wizard 1480® Wallac, Turku, Finland). Data were corrected for background radiation, cross over, dead time, and decay due to the collection times of the individual samples. A final normalization of the injected activity was calculated with the normalized blood tracer concentration and expressed as percent injected activity per mL (%IA/mL).

Biodistribution

Distribution of radioactivity in various organs was measured using count rates in regions of interest (ROIs) defined on serial planar scans. A baseline scan was performed within 1 h from activity infusion prior to first urination. Data were expressed as percentage of the whole body count fraction of injected activity (FIA).

Since data from one patient was not eligible for biodistribution, statistics were based on 19 patients. Time-activity-curves were drawn for visually well-defined GD2 positive tumors (FIA of tumor per mL, n=12 patients).

Bone marrow dose

The bone marrow dose was calculated using the following equation (*20*):

$$bone\ marrow\ dose\ \left[\frac{mGy}{MBq}\right] = 0.058 * \tilde{A}_{blood} * m_{RM} * \frac{RMECFF}{(1 - HCT) * A_{injected}}$$

Where $\tilde{A}_{blood}$ denotes accumulated blood activity concentration (MBq*h/g), m_{RM} denotes mass of red bone marrow (g) and $A_{injected}$ denotes the injected activity (MBq). RMECFF is red marrow extracellular fluid fraction and HCT denotes hematocrit.

The red bone marrow mass (m_{RM}) (g) was calculated from total body weight (g) multiplied by 1.37% in males and 1.16% in females (*21*). Dose conversion factor RMECFF/(1-HCT) was assumed to be 0.32 (*20*).

Dosimetry

Whole body, heart, lungs, liver, spleen, and kidney radiation absorbed doses were calculated from Iodine-131 time-integrated activity coefficent (TIAC)s in the defined region of interest (ROI). Organ radioactivity content was estimated from the geometric mean (GM) of anterior and posterior ROI counts. A standard marker of ^{131}I-GD2-ch14.18 (~1 MBq) was placed in each whole body scan as a reference to ensure constancy of

gamma camera electronics and scan speed. These data were fitted to a rising and falling exponential function:

$Y(t) = A\,[1-\exp(-\alpha t)] \cdot \exp(-\beta t)$

Integration of equation for Y(t) yields the cumulative activity in counts*h (or FIA*h). Finally Olinda® software (Vanderbilt University, Nashville, TN, USA, 2003) was used for dosimetric analysis of all patients.

Tumor uptake and tumor TIACs

Absorbed doses of tumors were calculated from ROIs with background correction and tumor volumes measured from CT or MRT scans. In patients presenting with multiple tumor lesions, a reference tumor site was defined based on CT or MRI data comprising the best delineated or largest lesion. Time-activity-curves presented an increasing behaviour in tumor regions during the examination cycle and this means the above described equation could not be applied for tumor TIAC. For this reason, we used the following formula for the TIAC in tumor regions:

$\tau_{tumor} = \tilde{A}_{tumor} / A_{injected}$ and

$$\tilde{A}_{Tumor} = \int_0^{\infty} dt\, A(t) = \int_0^{T} dt\, A(t) + \int_T^{\infty} dt\, A(t)$$

Where the first integral was approximated from experimental data using the trapezoidal rule and the second integral was analytically solved using the last measured value and a monoexponential “decay” with physical half-life time.

Statistics

Results are demonstrated as means ± standard deviation (SD). Data were calculated using Excel® software. Statistical test (one-way Anova) was performed using the Sigmastat® software (Version 3.5). For analyzing significance of the results, a t-test based on range was used. $p < 0.05$ was regarded as significant.

RESULTS

Biodistibution

Application of ^{131}I-GD2-ch14.18 was accompanied by a sensation of mild to moderate malaise and tightness in the chest during infusion in the majority of patients (18/20). In addition, Grade 3 generalized pains were observed in 2 cases (patient No. 3 and 17). These side effects were completely resolved right after the end of infusion in all cases. All patients received sequential WB scintigraphy scan up to d4. Data from 3 patients were not sufficient for dosimetry due to missing scan at d1 (patient No. 7) or having only 2 consecutive scans (patient No.8 and 20). Thus, scans from 17 individuals were used for dosimetric analyses. The tumor targeting rate on a per-patient base was 65% (13/20). In particular, 6/9 investigated patients suffering from NB showed uptake of ^{131}I-GD2-ch14.18. Clinical characteristics and tumor detectability on GD2-scans are depicted in Table 1. The liver and spleen were visualized in all patients except for one with a history of splenectomy. The urinary bladder showed pronounced radioactivity in most patients, usually on d1 and d2. No remarkable uptake was seen in the bone marrow compartment or in the kidneys at any time point.

Blood activity concentration in 3 adults indicated a nearly complete retention of ^{131}I-GD2-ch14.18 in the blood compartment up to 2 h after infusion (0.0174%±0.0018% IA/mL at 0.1 h p.i.) followed by a decrease with an effective blood half-life of approximately 24 h (Fig.1.A). Data from a single paediatric patient (Fig.1.B) showed a higher blood activity right after the tracer application (0.053% IA/mL) and an effective blood half-life of 41 h.

A typical example of sequential planar WB- scans is depicted in Fig. 2. Analysis of biodistribution (Fig. 3) demonstrated that the activity of ^{131}I-GD2-ch14.18 in organs reached a maximum within the first hour and continually declined thereafter (1 h p.i.: lung 8.02±1.17%, liver 9.33±1.63%, spleen 2.07±0.64 %, and kidney 2.24±0.91% vs. 24 h p.i.: lung 5.20±1.24%, liver 5.39±1.42%, spleen 1.25±0.42 %, and kidney 1.21± 0.61%). Tumor lesions showed uptake in 13/20 patients but a sole pelvic tumor lesion in patient No. 16 was partly superimposed by the urinary bladder. Hence, tumor dosimetry could be performed in n=12 patients.

In contrast, GD2-expressing tumors showed no early peak but a more stable activity level with maximum uptake between 1 and 3 days after injection (0.60±0.85% 1 h p.i., 0.52±0.65% 24 h p.i., 0.54±0.69% 48 h p.i., and 0.52±0.63% 72 h p.i.) (Fig. 3). Of note, the tumoral activity varied over a wide range between individuals (Fig. 4). Due to high blood pool activity level on early scans, tumor to background contrast was best on d2 or later.

Dosimetry

Quantification of radiation absorbed dose is presented in Table 2. The calculated median and mean doses to tumor lesions were 9.08 and 11.83 mGy/MBq, respectively. The ratios of median tumor to organ doses were 10.32 for lungs, 15.93 for liver, 7.90 for spleen, 15.93 for the kidneys, and 75.67 for the red bone marrow. The individual tumor absorbed dose varied over a range between 0.52 and 30.20 mGy/MBq. The noticeably highest and lowest values were both from Ewing´s sarcoma patients. All 6 GD2-positive NB patients showed intense uptake with a median tumor dose of 8.50 mGy/MBq.

Radioimmunotherapy (RIT)

Two adult patients (patient No. 1 with NB and patient No. 2 with pheochromocytoma) that showed an intense tumor uptake (tumor dose: 6.7 and 8.2 mGy/MBq) were selected to receive RIT with I-GD2-ch14.18. The bone marrow dose was calculated at 0.11 and 0.18 mGy/MBq, respectively. An activity of 2.3 and 2.9 GBq (30-40 MBq/kg) of I-GD2-ch14.18 was applied for RIT. Treatment was well tolerated in both cases. Both patients received posttherapeutic imaging with WB scans and additional SPECT/CT. Fig. 5 depicts intense targeting of bone and liver tumor lesions in the patient with NB on d 2 after RIT.

Follow-up image after 2 months (CT or MRT) showed a stable disease with metastases in the patient with NB. Moderate thrombocytopenia was observed 4 weeks after RIT and spontaneously recovered after another 4 weeks. However, the patient with pheochromocytoma presented with progression of metastases in the bone, bone marrow, liver, and lung 2 months after RIT. Pancytopenia with severe thrombocytopenia (19000/μL) occurred in this patient 6 weeks after RIT. Improvement thereafter indicates possible causality of RIT. Underlying limited hematopoiesis due to heavy pretreatment as well as bone marrow tumor involvement were likely cofactors. Overall survival of these patients was 17 and 6 months from RIT, respectively.

DISCUSSION

Even though radionuclide therapies such as MIBG or peptide receptor radionuclide therapy (PRRT) are readily available for NB or NET, patients with insufficient targeting or refractory disease may be candidates for GD2-directed RIT. Immunotherapy targeting

GD2 using the chimeric antibody ch14.18 has been studied extensively, but its use as a radiolabeled compound and thus dosimetry in humans as a prerequisite for RIT have been lacking so far. Our results confirmed significant GD2 targeting in the majority of tumors investigated. In particular, the greater part of patients with advanced NB showed intense tumor uptake. These results correspond to the findings of Reuland et al. (*22*) who revealed GD2 targeting in a cohort of largely MIBG-negative NBs using the same antibody but labelled with ^{99m}Tc. GD2 targeting was currently also demonstrated in 2 individuals with osteosarcoma and 3/6 patients with Ewing´s sarcomas which is in keeping line with the variable expression of the target antigen in these malignancies (*23*). Overall, our study revealed that the ch14.18 antibody retains its antigen-binding ability after labeling with iodine-131.

Serial WB scans showed a slow but continuous decline of organ and blood radioactivity while GD2-positive tumor lesions demonstrated relatively stable radiotracer retention over time. This resulted in good tumor to background contrast from 2 days after tracer injection. Slow clearance of radioactivity from the blood is common for radiopharmaceuticals based on full-size monoclonal antibodies (*24*) and has in fact been observed previously with ^{64}Cu-labeled GD2-ch14.18 antibody in an animal model (*25,26*). The prolonged blood residence of the antibody conjugate will contribute to absorbed dose in blood-bearing organs such as the liver, spleen, heart, kidneys, and bone marrow. Nevertheless, dosimetry in GD2-positive tumors revealed 10-fold higher or even better tumor to organ dose ratios i.e. therapeutic indices, thus meeting published criteria for RIT (*12*).

Despite premedication, mild to moderate antigen reactions were observed under infusion of I-GD2-ch14.18 in the majority of our patients while 2 individuals additionally

suffered from diffuse pain. Such antigen toxicity is well known from therapeutic application of non-radioactive GD2-targetting antibodies (*27*) and has been shown to be dose dependent (*28*). However, the amount of antibody injected for scintigraphy (max. 1 mg) was less than 10 % of the approved dose in non-radioactive immunotherapy with Dinutuximab.

Our study has some limitations: Only planar scintigraphy was available for sequential imaging while SPECT/CT was added only in selected cases aiming to better delineate tumor sites. As a result, dose estimations are based on planar scans alone and have to be considered merely semi-quantitative, as the combined uncertainties are considered a factor 2 or even greater (*29*). Moreover, overlap of lesions and blood pool or organs may prevent precise identification of tumor lesions. A dual integral formula was used to estimate tumor TIAC. Because effective half-life after the last measured time point was unknown, physical decay was used for the second integral. As a result, the true tumor absorbed dose might be considerably lower. Obviously, an elaborate dosimetry will be needed for volume of interest analyses using quantitative SPECT/CT (*30*) or PET/CT (*25*). Serial blood samples were only available in 4/20 patients, thus analysis of ^{131}I-GD2-ch14.18 blood kinetics and red marrow dose are to be regarded as preliminary. Finally, due to the small number of patients in this retrospective analysis, tumor targeting and especially safety and efficacy of ^{131}I-GD2-ch14.18 RIT will have to be further evaluated in prospective studies.

CONCLUSION

Sequential scintigraphy demonstrated slow clearance of the ^{131}I-GD2-ch14.18 from blood resulting in favorable tumor to background contrast from 2 days after application.

With an acceptable red marrow dose, RIT may be considered as an option for patients with high tumor uptake. Because of the variable GD2-expression, pretherapeutic imaging and dosimetry are recommended. Development of GD2-targeting fragments might accelerate blood clearance and may improve RIT in the future.

DISCLOSURE

Funded by the Deutsche Forschungsgemeinschaft (DFG, German Research Foundation) under Germany's Excellence Strategy - EXC 2180 – 390900677.

No other potential conflict of interest relevant to this article was reported.

KEY POINTS

QUESTION:

What is the tumor targeting and biodistribution of ^{131}I-GD2-ch14.18 in patients with late-stage disease that are potentially eligible for radioimmunotherapy?

PERTINENT FINDINGS:

In this retrospective study sequential scintigraphy demonstrated a favorable tumor to background contrast of the ^{131}I-GD2-ch14.18 from 2 days after application. Moreover, dosimetry in planar scintigraphy in GD2-positive tumors revealed up to 10-fold higher tumor to organ dose ratios i.e. therapeutic indices.

IMPLICATIONS FOR PATIENT CARE:

With an acceptable red marrow dose, RIT may be an option for patients with high tumor uptake. Because of the variable GD2-expression, pretherapeutic imaging and dosimetry are recommended.

REFERENCES

1. Mujoo K, Cheresh DA, Yang HM, Reisfeld RA. Disialoganglioside GD2 on human neuroblastoma cells: target antigen for monoclonal antibody-mediated cytolysis and suppression of tumor growth. *Cancer Res.* 1987;47:1098-1104.

2. Schulz G, Cheresh DA, Varki NM, Yu A, Staffileno LK, Reisfeld RA. Detection of ganglioside GD2 in tumor tissues and sera of neuroblastoma patients. *Cancer Res.* 1984;44:5914-5920.

3. Svennerholm L, Bostrom K, Fredman P, et al. Gangliosides and allied glycosphingolipids in human peripheral nerve and spinal cord. *Biochim Biophys Acta.* 1994;1214:115-123.

4. Chang HR, Cordon-Cardo C, Houghton AN, Cheung NK, Brennan MF. Expression of disialogangliosides GD2 and GD3 on human soft tissue sarcomas. *Cancer.* 1992;70:633-638.

5. Navid F, Santana VM, Barfield RC. Anti-GD2 antibody therapy for GD2-expressing tumors. *Curr Cancer Drug Targets.* 2010;10:200-209.

6. Ploessl C, Pan A, Maples KT, Lowe DK. Dinutuximab: An anti-GD2 monoclonal antibody for high-risk neuroblastoma. *Ann Pharmacother.* 2016;50:416-422.

7. Ladenstein R, Potschger U, Valteau-Couanet D, et al. Interleukin 2 with anti-GD2 antibody ch14.18/CHO (dinutuximab beta) in patients with high-risk neuroblastoma (HR-NBL1/SIOPEN): a multicentre, randomised, phase 3 trial. *Lancet Oncol.* 2018;19:1617-1629.

8. Yu AL, Gilman AL, Ozkaynak MF, et al. Anti-GD2 antibody with GM-CSF, interleukin-2, and isotretinoin for neuroblastoma. *N Engl J Med.* 2010;363:1324-1334.

9. Dinutuximab approved for high-risk neuroblastoma. *Cancer Discov.* 2015;5:OF5.

10. Ehlert K, Hansjuergens I, Zinke A, et al. Nivolumab and dinutuximab beta in two patients with refractory neuroblastoma. *J Immunother Cancer.* 2020;8:e00540.

11. Gohil K. Pharmaceutical approval update. *P t.* 2015;40:327-360.

12. Larson SM, Carrasquillo JA, Cheung NK, Press OW. Radioimmunotherapy of human tumours. *Nat Rev Cancer.* 2015;15:347-360.

13. Kaminski MS, Zelenetz AD, Press OW, et al. Pivotal study of iodine I 131 tositumomab for chemotherapy-refractory low-grade or transformed low-grade B-cell non-Hodgkin's lymphomas. *J Clin Oncol.* 2001;19:3918-3928.

14. Witzig TE, Gordon LI, Cabanillas F, et al. Randomized controlled trial of yttrium-90-labeled ibritumomab tiuxetan radioimmunotherapy versus rituximab immunotherapy

for patients with relapsed or refractory low-grade, follicular, or transformed B-cell non-Hodgkin's lymphoma. *J Clin Oncol.* 2002;20:2453-2463.

15. Cheung NK, Kushner BH, LaQuaglia M, et al. N7: a novel multi-modality therapy of high risk neuroblastoma (NB) in children diagnosed over 1 year of age. *Med Pediatr Oncol.* 2001;36:227-230.

16. Cheung NK, Cheung IY, Kushner BH, et al. Murine anti-GD2 monoclonal antibody 3F8 combined with granulocyte-macrophage colony-stimulating factor and 13-cis-retinoic acid in high-risk patients with stage 4 neuroblastoma in first remission. *J Clin Oncol.* 2012;30:3264-3270.

17. Maxon HR, Thomas SR, Hertzberg VS, et al. Relation between effective radiation dose and outcome of radioiodine therapy for thyroid cancer. *N Engl J Med.* 1983;309:937-941.

18. Press OW, Eary JF, Appelbaum FR, et al. Radiolabeled-antibody therapy of B-cell lymphoma with autologous bone marrow support. *N Engl J Med.* 1993;329:1219-1224.

19. Ozkaynak MF, Gilman AL, London WB, et al. A comprehensive safety trial of chimeric antibody 14.18 with GM-CSF, IL-2, and Isotretinoin in high-risk neuroblastoma patients following myeloablative therapy: children's oncology group study ANBL0931. *Front Immunol.* 2018;9:1355.

20. Stabin MG, Siegel JA, Sparks RB. Sensitivity of model-based calculations of red marrow dosimetry to changes in patient-specific parameters. *Cancer Biother Radiopharm.* 2002;17:535-543.

21. Woodard HQ. The relation of weight of haematopoietic marrow to body weight. *Br J Radiol.* 1984;57:903-907.

22. Reuland P, Geiger L, Thelen MH, et al. Follow-up in neuroblastoma: comparison of metaiodobenzylguanidine and a chimeric anti-GD2 antibody for detection of tumor relapse and therapy response. *J Pediatr Hematol Oncol.* 2001;23:437-442.

23. Dobrenkov K, Ostrovnaya I, Gu J, Cheung IY, Cheung NK. Oncotargets GD2 and GD3 are highly expressed in sarcomas of children, adolescents, and young adults. *Pediatr Blood Cancer.* 2016;63:1780-1785.

24. Lewis MR, Wang M, Axworthy DB, et al. In vivo evaluation of pretargeted 64Cu for tumor imaging and therapy. *J Nucl Med.* 2003;44:1284-1292.

25. Dearling JL, Voss SD, Dunning P, et al. Imaging cancer using PET--the effect of the bifunctional chelator on the biodistribution of a (64)Cu-labeled antibody. *Nucl Med Biol.* 2011;38:29-38.

26. Maier FC, Schmitt J, Maurer A, et al. Correlation between positron emission tomography and Cerenkov luminescence imaging in vivo and ex vivo using 64Cu-labeled antibodies in a neuroblastoma mouse model. *Oncotarget.* 2016;7:67403-67411.

27. Dobrenkov K, Cheung NK. GD2-targeted immunotherapy and radioimmunotherapy. *Semin Oncol.* 2014;41:589-612.

28. Cheung NK, Kushner BH, Cheung IY, et al. Anti-G(D2) antibody treatment of minimal residual stage 4 neuroblastoma diagnosed at more than 1 year of age. *J Clin Oncol.* 1998;16:3053-3060.

29. Stabin MG. Uncertainties in internal dose calculations for radiopharmaceuticals. *J Nucl Med.* 2008;49:853-860.

30. Cheal SM, Xu H, Guo HF, et al. Theranostic pretargeted radioimmunotherapy of internalizing solid tumor antigens in human tumor xenografts in mice: Curative treatment of HER2-positive breast carcinoma. *Theranostics.* 2018;8:5106-5125.

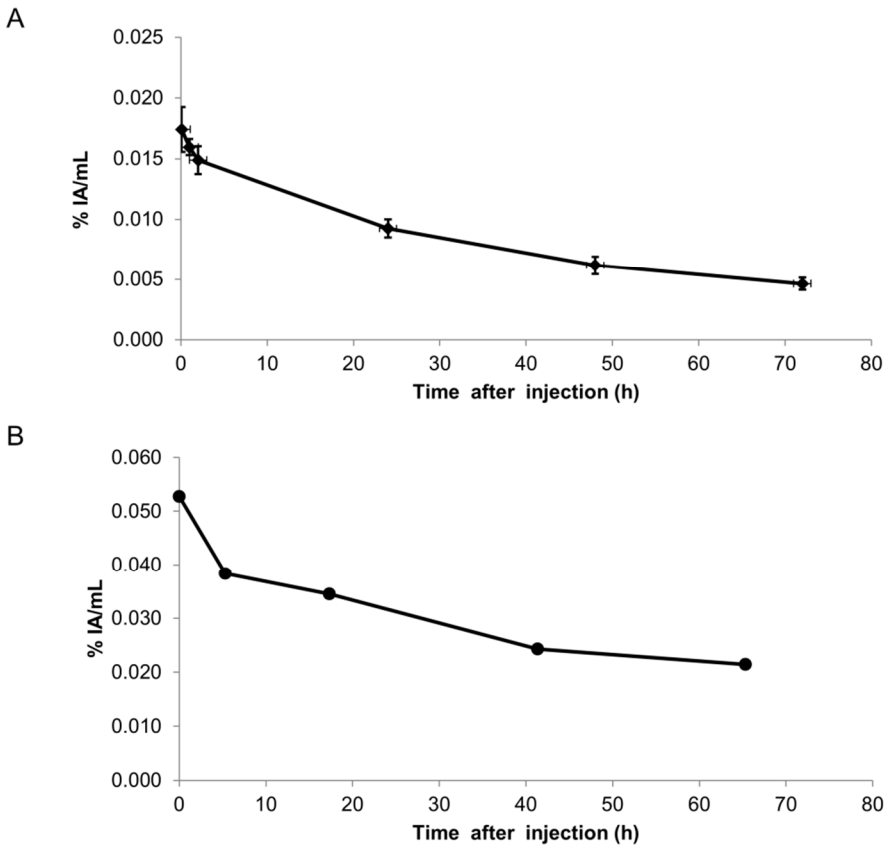

FIGURE 1. Normalized blood tracer concentrations at different time points (percentage of the injected activity of ^{131}I-GD2-ch14.18 per mL blood, % IA/mL). (A) Data represent mean±SD from 3 adults (patient No. 1, 2, 3). (B) Values from one paediatric patient (6-year-old boy, patient No. 4).

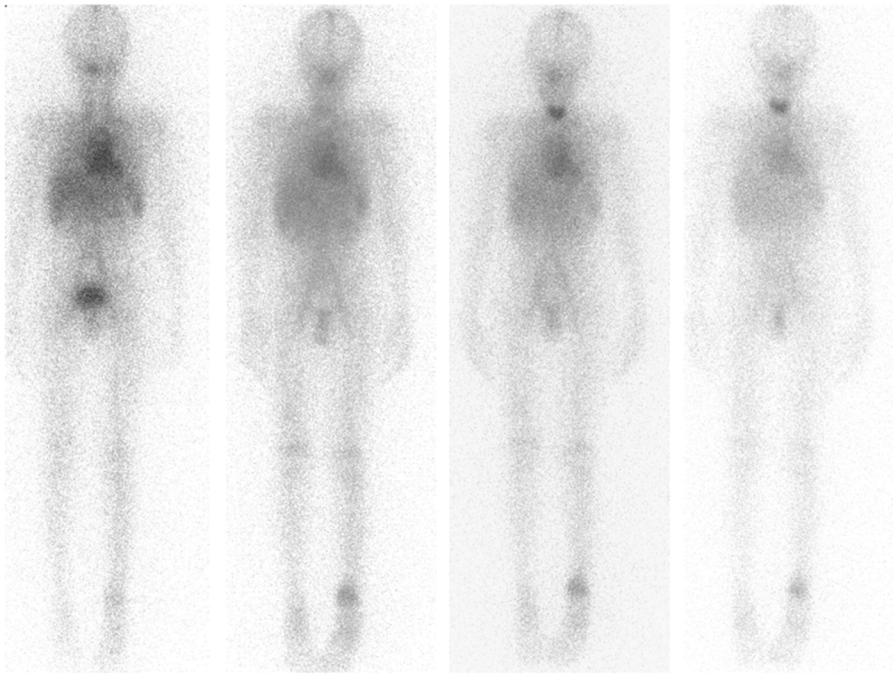

FIGURE 2. Sequential planar WB-^{131}I-GD2-ch14.18-scans (anterior view) demonstrating increased targeting of a tumor lesion in the left distal tibia on day 2-4 in a patient with osteosarcoma (No.18).

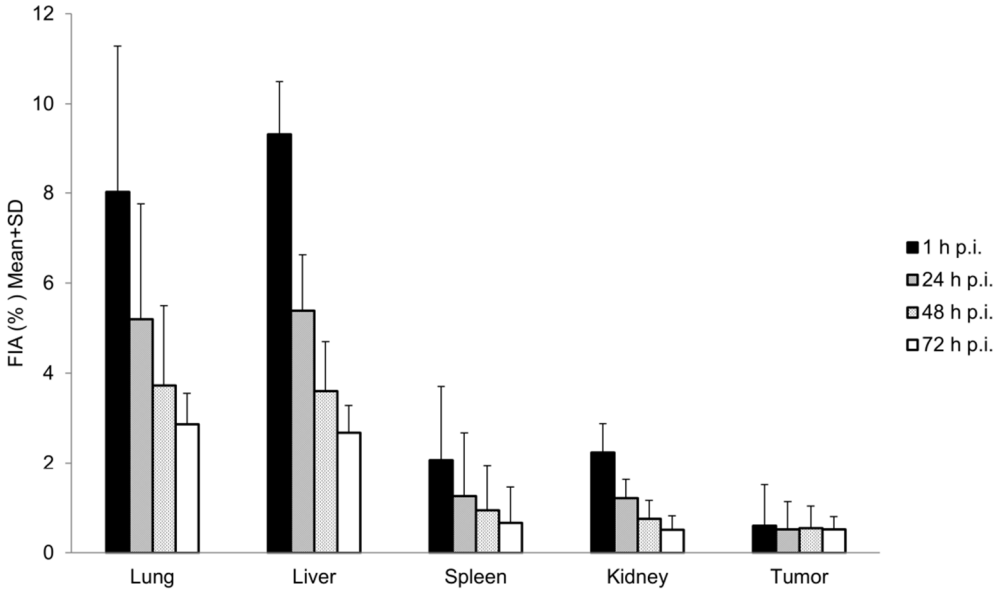

FIGURE 3. Biodistribution as calculated from ROI analysis of planar scintigraphy (n=19): ^{131}I-GD2-ch14.18 uptake in organ and tumor lesions is expressed as fraction of injected activity (FIA) (mean±SD) at different time points.

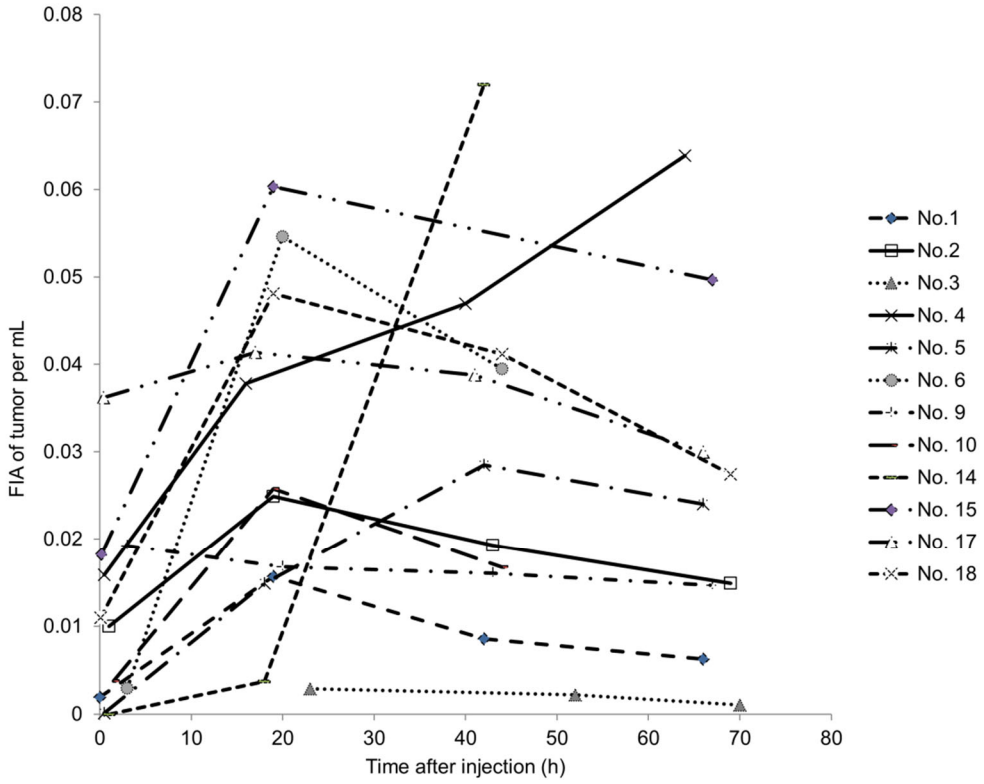

FIGURE 4. Time-activity curves for GD2 positive tumors (FIA of tumor volume per mL). Data represent uptake of reference tumor lesions in 12 patients. Due to overlapping of tumor lesion with urinary bladder, patient No.16 was excluded.

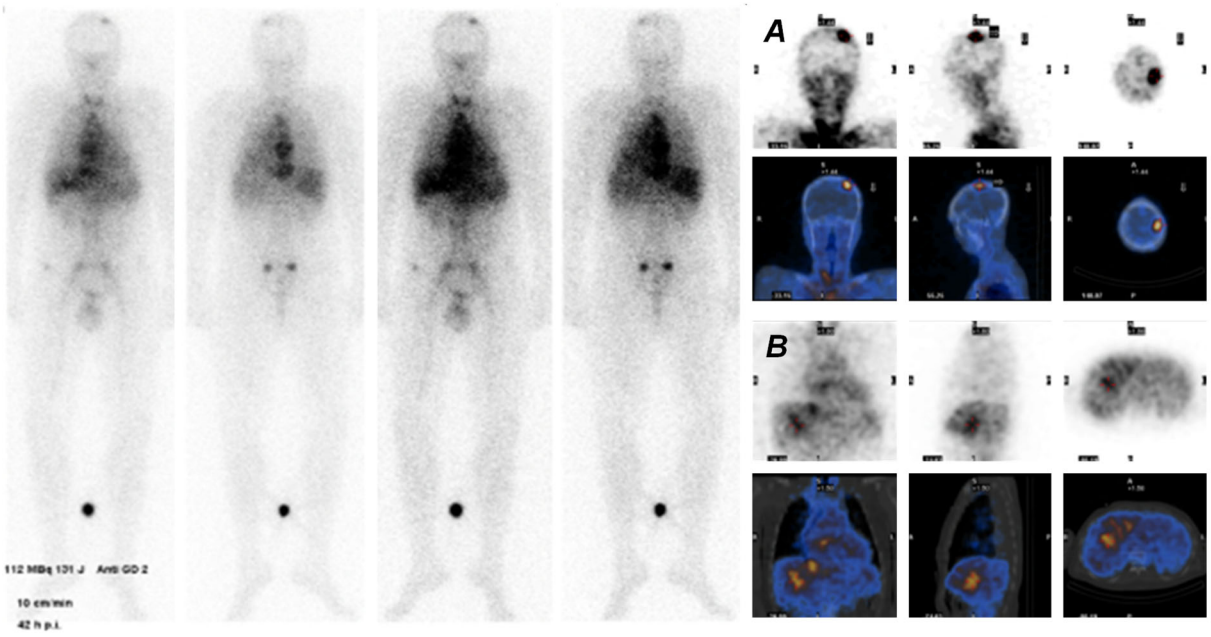

FIGURE 5. ^{131}I- GD2-ch14.18 scan with additional SPECT/CT on day 2 from application demonstrates intense targeting of bone (*A*) and liver (*B*) tumor lesions in a patient with NB (patient No.1).

TABLES

TABLE 1. Patient characteristics, ^{131}I-GD2-ch14.18 activity and tumor detectability on GD2-scans.

Patient No.	Gender	Age (years)	BMI	Histology	Prior Treatments	Histology and MIBG scan	Tumor sites	Activity (MBq)	Tumor Detection
1	M	23	21	neuroblastoma	S, chemo, RT	G3, MIBG NEG	Bone, Hep, Lym	82.3	POS
2	M	32	23	pheochromocytoma	S, chemo, RT, PRRT	Chromogranine POS	Bone, Hep, Pul	89.7	POS
3	F	50	21	NET	chemo, RT	Chromogranine POS	Bone, Hep, Lym, Pul	87.2	POS
4	M	7	13	neuroblastoma	S, chemo, RT, ABMT	MIBG NEG, VMA/HVA NEG, MYCN POS	Bone	50.8	POS
5	F	8	16	neuroblastoma	S, chemo, RT, ABMT	MIBG, NSE,VMS, MYCN NEG	Bone, BM	32.6	POS
6	M	8	16	neuroblastoma	S, chemo, RT, ABMT	MYCN NEG, no chromosome aberration 1 (p36)	Bone	27	POS
*7	M	7	14	neuroblastoma	S, chemo, RT, ABMT, GD2	MYCN NEG, MIBG POS	Bone, BM	24.7	NEG
*8	M	4	16	neuroblastoma	S, chemo, MIBG, ABMT	MYCN NEG, imbalance Chromosome 1 (p36).	Bone, BM	21.2	NEG
9	F	4	13	neuroblastoma	S, chemo, RT, ABMT	MIBG NEG	Bone, Lym	22.3	POS
10	F	13	15	neuroblastoma	S, chemo, MIBG, ABMT, GD2	MYCN NEG, 1 p-Deletion POS, catecholamine POS, MIBG POS	Bone, BM	46.8	POS
11	M	51	29	Ewing´s sarcina	S, chemo, RT, ABMT	Ewing's sarcoma	Cerebral, Pul	83.2	NEG
12	F	20	19	Ewing´s sarcina	S, chemo, RT, ABMT	Ewing's sarcoma	Hep, Pul	59	NEG
13	M	18	30	Ewing´s sarcina	S, chemo	Ewing's sarcoma	Pul	130.8	NEG
14	M	13	25	Ewing´s sarcina	S, chemo, RT, ABMT	Ewing's sarcoma	Bone, Pul	76.5	POS
15	M	17	18	Ewing´s sarcina	S, chemo, ABMT	Ewing's sarcoma	Bone, Lym	80.5	POS
16	F	18	27	Ewing´s sarcina	S, chemo, RT, ABMT	Ewing's sarcoma	Bone	79.5	POS
17	M	19	19	osteosarcoma	S, chemo	osteosarcoma	Bone, Lym, Pul, Soft	82.1	POS
18	M	11	19	osteosarcoma	S, GD2	osteosarcoma	no metastasis	84	POS
19	M	22	17	osteosarcoma	S, chemo	osteosarcoma	GI, Pul	105	NEG
*20	M	5	17	neuroblastoma	S, chemo, RT, ABMT	MYCN and MIBG Neg, no chromosome aberration 1 (p36)	Bone, BM, Lym	59.3	NEG

Abbreviations: S, surgery; chemo, chemotherapy; RT, focal radiotherapy; ABMT, myeloablative chemotherapy with stem-cell rescue; NEG, negative; GD2, non-radioactive GD2-antibody therapy; MIBG, ^{131}I-MIBG-therapy; POS, positive; Bone, skeletal metastases; BM, bone marrow metastases; GI, gastrointestinal tract metastases; Hep, hepatic metastases; Lym, lymph nodes metastases; PRRT, peptide receptor radiotherapy; Pul, pulmonary metastases; Soft, soft tissue metastases.

*, not suitable for dosimetric analysis.

TABLE 2. ^{131}I-GD2-ch14.18 absorbed dose (mGy/MBq).

Target organ	Median	Min.	Max.	n	Mean	SD
Red marrow	0.12	0.09	0.18	4	0.12	0.03
Lung	0.88	0.29	3.31	17	1.20	0.86
Liver	0.57	0.23	1.70	17	0.70	0.41
Spleen	1.15	0.40	4.41	16	1.51	1.13
Kidney	0.57	0.19	1.89	17	0.72	0.48
Total body	0.30	0.09	1.46	17	0.41	0.34
Tumor	9.08	0.52	30.20	12	11.83	8.10
Effective dose	0.43	0.12	2.68	17	0.61	0.59

Graphical Abstract